JOURNAL OF PROPULSION AND POWER
Vol. 19, No. 4, July–August 2003

Numerical Simulation of Ion Beam Optics for Multiple-Grid Systems

Yoshinori Nakayama*
National Defense Academy, Kanagawa 239-8686, Japan
and
Paul J. Wilbur†
Colorado State University, Fort Collins, Colorado 80523-1374

A high specific impulse ion thruster operated at a voltage of 10 kV has been studied, and the problems of direction impingement on the accelerating grid and charge-exchange ion production and impingement have been considered. These problems are addressed by considering the use of four or more grids (multiple-grid system). To evaluate these multiple grid systems, a three-dimensional particle simulation code that employs 1) an energy compensation method, 2) a simplified sheath definition method, and 3) a high-speed coding was developed. It was confirmed that results from this simulation are obtained at a high-speed and are in good agreement with experimental data. With use of this code, several multiple-grid systems were evaluated.

Nomenclature

a	=	acceleration
h	=	length between mesh points
I	=	current
m	=	mass
n	=	number density
q	=	charge density
r, z, θ	=	cylindrical coordinate
t	=	time
V	=	voltage
v	=	velocity
x, y	=	Cartesian coordinate
ε	=	dielectric constant
ϕ	=	electric potential
σ	=	cross section

Subscripts

ac	=	accelerating grid
b	=	beam
c	=	charge-exchange reaction
fast	=	fast particle
i	=	ion
n	=	neutral
N	=	net
p	=	plasma
SCLC	=	space charge limited current
slow	=	slow particle

Introduction

THERE is need for propulsion systems that operate longer, have greater total impulse capabilities, and can thereby accommodate the natural trend of spacecraft missions to become more ambitious. Because the propulsion system generally does not capture its propellant in space, the propellant that can be used is limited to that loaded initially. This mission trend translates, in turn, to a corresponding need for ion thrusters that will make most effective use of the propellants they carry, that is, will operate at increasingly higher specific impulses.

Generally, an ion thruster has a two- or three-grid system and operates at a net accelerating voltage of the order of 1 kV (a specific impulse near 3000 s). Increasing this voltage increases specific impulse, in proportion to its square root. For the work described herein, a high specific impulse ion thruster (HiIsp-IT) operated at a voltage of 10 kV has been studied, and the problems of direct ion impingement on the accelerating grid and charge-exchange ion production and impingement have been considered. These phenomena lead to sputter erosion and sputter coating effects that pose problems because they can limit thruster lifetime as a result of wear and electrical breakdown, respectively.

These problems, which might be expected to worsen because of the high voltages involved, are addressed in this study by considering the use of four or more grids, that is, multiple-grid systems. Each of these grids can be biased in various ways to accomplish precise control of ion beam trajectories for the mitigation of the aforementioned problems. Furthermore, a grid system has many design parameters, for example, number of electrodes, thickness, aperture diameter, gap, etc. Because of the large number of parameters involved, the design of a multiple-grid system is best accomplished using high-speed numerical analysis to guide an experimental study that would otherwise be time consuming and costly.

Much numerical simulation of ion beam optics has already been done by Whealton et al.,[1] Hayakawa,[2] and others.[3–6] The OPT code developed by Arakawa and Ishihara[7] is a well-known code used for simulation of ion beam optics. It can be used for high-speed analysis of conventional ion thruster two- or three-grid systems, and it has typically yielded results that agree reasonably well with experimental results.[3] To evaluate the HiIsp-IT grid system, in this study, this code was modified so that it could be used to simulate multiple-grid systems and model charge-exchange phenomena.

In addition, another high-speed simulation code (igx) was developed. This was done when it was determined that more accurate simulations of the ion extraction and acceleration processes than those obtained from OPT are needed for HiIsp-IT applications. The igx code simulates both the behavior of beam ions and charge-exchange ion phenomena.

The objectives of this study are 1) modification of OPT code and development of the igx code to enable investigation of multiple-grid systems, 2) comparative evaluation of these codes with each other and with experimental data, and 3) simulation and discussion of several multiple-grid options for HiIsp-IT applications.

Received 29 March 2002; revision received 2 December 2002; accepted for publication 3 March 2003.

*Research Associate, Department of Aerospace Engineering, 1-10-20 Hashirimizu, Yokosuka; ynakayam@nda.ac.jp. Member AIAA.

†Professor, Department of Mechanical Engineering; pwilbur@engr.colostate.edu. Member AIAA.

OPT Code

The OPT code,[7] which simulates ion thruster beam optics, employs a two-dimensional cylindrical coordinate system. The shape and position of the bounding ion extraction surface or sheath, which is known to have a critical influence on ion optical behavior, is modeled in the code using a cubic function. Ions are extracted from this surface, accelerated through the potential difference between the screen and accelerating grids, and delivered to a downstream boundary. Some ions impact on the acceleration grid as an impingement current. The electrical potential ϕ of each mesh point within the grid-system region is calculated using Poisson's equation:

$$\nabla^2\phi = -q/\varepsilon \tag{1}$$

The simultaneous equations associated with all of the mesh points are solved by the successive overrelaxation (SOR) method. Ion motion is described using the Runge–Kutta method. This code employs a flux-tube concept in which an ion is treated as a flux, and its charge is distributed to pairs of mesh points adjacent to its position at the end of each time interval. The sheath shape expressed in terms of cubic function coefficients is iterated until the ion current density to the sheath from the discharge plasma is equal to space-charge-limited current densities extracted over the sheath surface. Figure 1 is the flow chart for this code. Iteration takes place until the beam current I_b agrees with a value, I_{SCLC}, specified through an input perveance.

As part of this work, the code was modified so it could describe 1) ion flow through as many as five grids and 2) charge-exchange phenomena. The charge-exchange reaction describes a collision between a fast ion and a slow neutral in accordance with the following equation:

$$A^+_{\mathrm{fast}} + A_{\mathrm{slow}} \rightarrow A^+_{\mathrm{slow}} + A_{\mathrm{fast}}$$

The charge-exchange reaction rate $(\mathrm{d}n_c/\mathrm{d}t)$ of each cell (surrounded by eight mesh points) is calculated:

$$\frac{\mathrm{d}n_c}{\mathrm{d}t} = n_n n_i v_i \sigma_c(v_i) \tag{2}$$

The number density of neutrals is determined using conductance values for the grids and assuming radially uniform free-molecular flow. The temperature of each grid is 500 K. Each charge-exchange ion is placed at the centerpoint of the cell in which it is produced and then moved to a boundary via the electrical field using the Runge–Kutta method. The influence of charge-exchange ions on the intragrid potentials is neglected.

This modified code, which is in Pascal, uses a memory-saving method and requires only the same 640-KB memory required by the original code. In addition, the code was modified so that potential data from a previous similar solution could be used to reduce the calculation time.

Simulation igx Code

The igx code simulates ion extraction through ion thruster grids in a three-dimensional, cylindrical coordinate system. It also simulates charge-exchange ion production and extraction in the same way the modified OPT code does. To reduce the execution time and describe ion motion more accurately, this code also integrates particle-in-cell (PIC), region sharing, and energy compensation concepts. Figure 2 shows the flow chart of the igx code.

Charge Distribution

Ion motion is determined using data from node point potentials, and the potentials are determined using Poisson's equation. For the first loop, the sheath is assumed to be at a flat boundary far upstream of the screen grid. The PIC method is used to distribute the charge of each ion to the eight mesh points that surround it at the conclusion of each time interval used in the analysis. The potentials at each node point are determined using the SOR method after the motions of all ions have been traced so that calculation times can be reduced.

Region Sharing

The ion optics simulation assumes the usual hexagonal arrangement of holes. Figure 3 shows the shape of the numerical space used in the code. Note that point A is a unique point that is common to all three holes that surround it. To reduce the calculation cost, the ion motion is described in the triangular column region OAC–O′A′C′, and the potential field is calculated within the cylindrical sector OAB–O′A′B′. Potentials in the column ABC–A′B′C′ are determined as a mirror reflection of those in the column ADC–A′D′C′ about the plane AC–A′C′. The ion motion is described in a three-dimensional Cartesian coordinate system to reduce the calculation cost further.

Energy Compensation

Particle motion is described in the code using the Euler method with the Courant condition applied. This is expressed in the

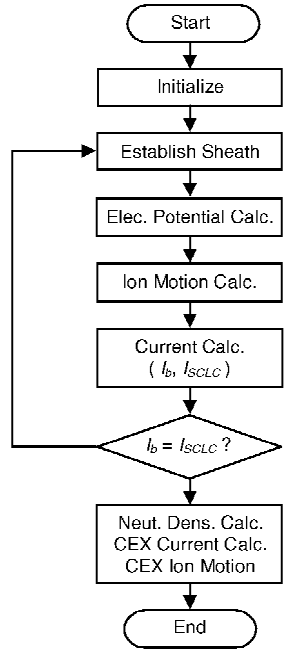

Fig. 1 Flow chart of OPT code.

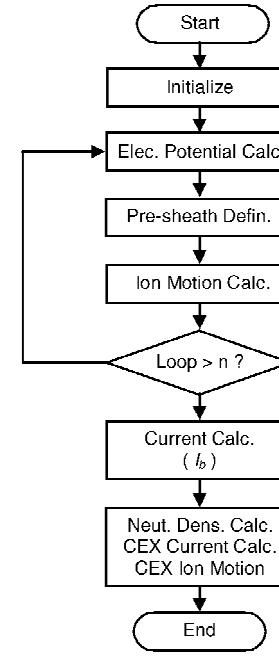

Fig. 2 Flow chart of igx code.

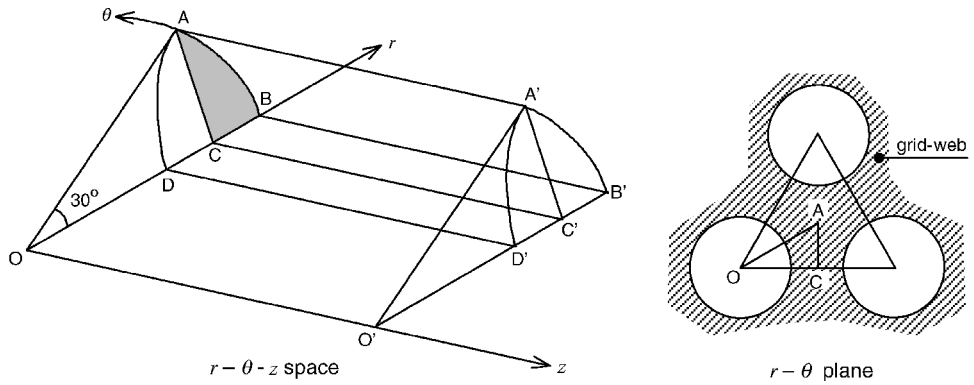

Fig. 3 Analysis space.

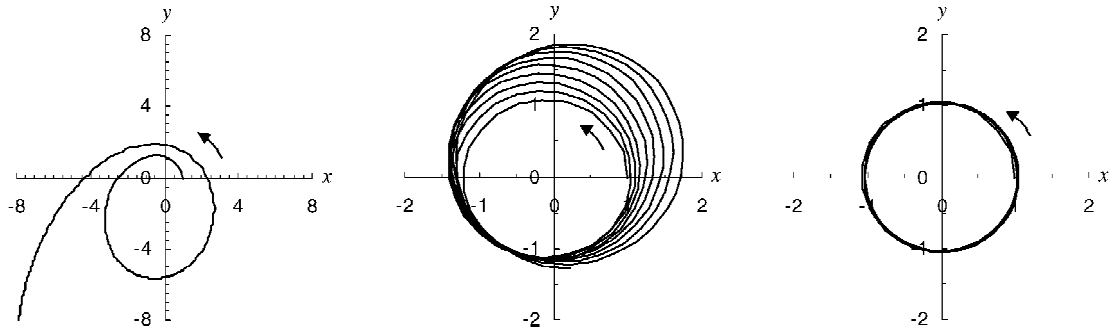

a) Euler method **b) Runge–Kutta method** **c) Energy-compensation method**

Fig. 4 Descriptions of uniform circular motion in Cartesian coordinates.

following equations:

$$v' = v + a\Delta t, \qquad x' = x + v\Delta t + \tfrac{1}{2}a\Delta t^2 \tag{3}$$

$$\Delta v \times \Delta t \leq \tfrac{1}{2}h \tag{4}$$

The Courant condition assures a precise description of particle motion, but it does not assure conservation of total energy, that is, potential plus kinetic energies, in accordance with the equation

$$q\phi + \tfrac{1}{2}mv^2 = \text{const} \tag{5}$$

Because the region sharing method is adopted in this code as already noted, the description of ion motion within the cell on/near the z axis, where the cell volume is small, is critical. To evaluate the accuracy of the method near the axis, uniform circular motion in a two-dimensional Cartesian coordinate system was simulated. Figure 4 illustrates the motion computed using three different numerical approaches. It is assumed for this comparison that there is a gravitational force acting on a mass from the z axis at $x = y = 0$. The conditions (initial velocity, gravitational force field, and time step) are the same for each approach. When the Euler method is used (Fig. 4a), rapid divergence is obvious, and when the Runga–Kutta method is used (Fig. 4b), divergence is still apparent even though the Courant condition was imposed. A precise description of ion motion is necessary in this simulation because this code deals with ions that experience a vast range of kinetic energies (over the order of magnitude range from 1 eV to 10 keV). In this simulation, therefore, compensation is applied to hold total ion energy constant at the conclusion of each interval of motion. The direction of the ion velocity vector is not changed, but its length is adjusted to satisfy Eq. (5). Although the momentum is not conserved when this method is used, the error in the momentum does not become substantial because the energy is conserved. This method has a kind of robustness. As shown in Fig. 4c, compensation in this way yields the best numerical simulation for the uniform circular motion problem. This method is preferred over the Runge–Kutta method not only because error accumulation is reduced via compensation, but also because it requires fewer calculation steps and is, therefore, faster and more efficient.

Note that the Symplectic method[8] developed in the 1990s is also conservative and efficient. In the present case, however, a preliminary feasibility study indicated it was unsuitable because of the large potential differences involved.

Sheath Definition

As suggested earlier, results obtained from optics simulations are strongly dependent on the shape of the ion extraction surface. In this simulation, a simple approach is used. The plasma upstream of the ion emitting sheath surface is described in terms of ions and electrons in equilibrium. The basic concept applied is suggested schematically in Fig. 5. It is assumed that the extreme left point, which is far upstream of the screen grid, is maintained at the discharge chamber plasma potential ϕ_p and that the potential of the other points as determined from the solution of the Laplace equation are as shown in Fig. 5a. Because ions are injected from the extreme left (plasma) plane, the potential of the points determined using Poisson's equation (1) will rise above ϕ_p, as shown in Fig. 5b. If the calculated potential is over plasma space potential, as shown in Fig. 5c, it is argued that these higher potentials would draw electrons (negative charges) from the adjoining plasma to maintain equilibrium. This causes the potentials to drop back to ϕ_p, as suggested in Fig. 5d. The mesh point at ϕ_p that is farthest downstream is called the plasma internal point, and the boundary connecting these points is designated the sheath in this study. Ions are extracted randomly from positions within the cells near the plasma internal points with an initial velocity determined by the Bohm condition. These ion extraction positions are determined by the requirement that the ion-induced potentials not exceed the plasma space potential. The process of computing the sheath location and shape is repeated using electrical potentials determined from the subsequent iterations of field calculations when ions are being emitted from the sheath. The iteration process under which the sheath surface evolves and

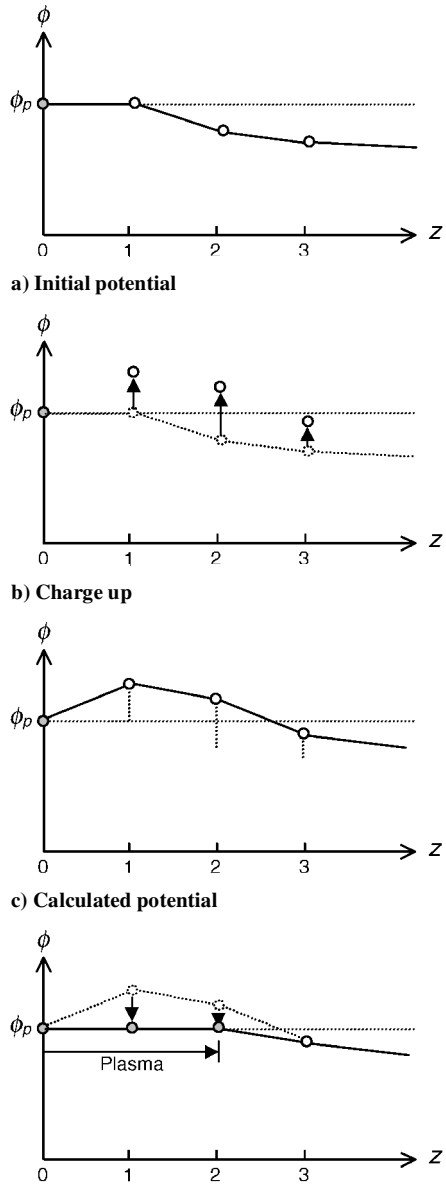

a) Initial potential

b) Charge up

c) Calculated potential

d) Potential adjustment

Fig. 5 Schematic of presheath definition.

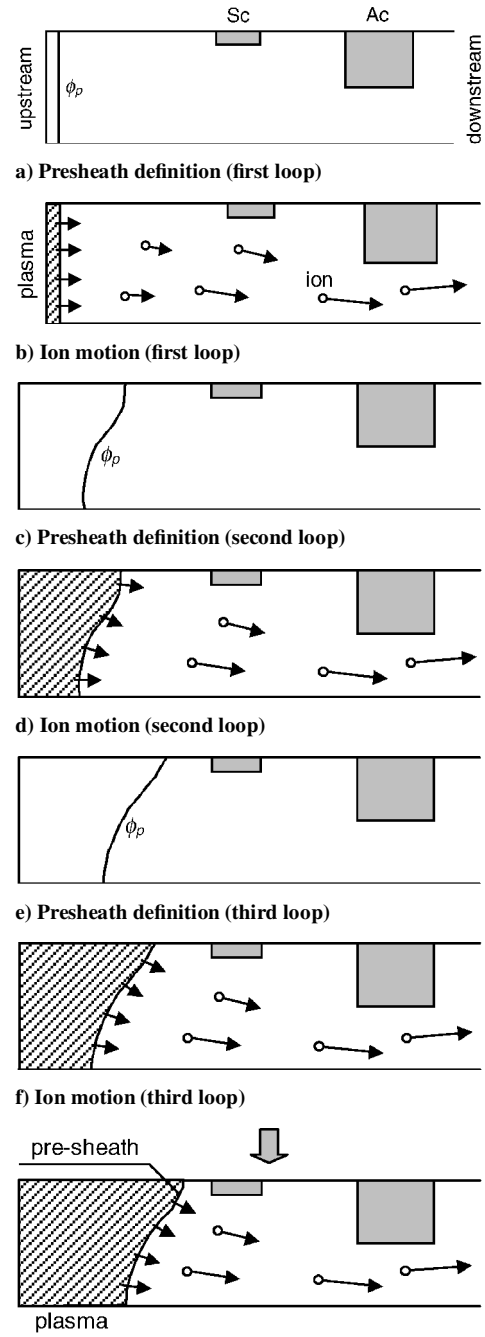

a) Presheath definition (first loop)

b) Ion motion (first loop)

c) Presheath definition (second loop)

d) Ion motion (second loop)

e) Presheath definition (third loop)

f) Ion motion (third loop)

g) Presheath definition and ion motion (final loop)

Fig. 6 Schematic of presheath development.

is coupled to the ion beam formation and acceleration processes is summarized in Fig. 6.

In a preliminary study, it was determined that the position and shape of the sheath surface was independent of the distance between the initial upstream boundary and the screen grid, that is, the line segment OA shown in Fig. 3, if this distance was greater than 1.5 times the radius OA.

High-Speed Coding

A kind of object-oriented coding, which requires a lot of memory but yields rapid, low-cost simulation, was used. To realize reasonable simulation times the igx code is typically run 14 times with 1000 ions to establish the nominal sheath shape and location and downstream potentials before it is run a final time with 10,000 ions to obtained the final solution. It was shown in preliminary study that the results obtained were independent of the number of iteration loops provided the number loops was over 15 (= 14 + 1) and the simulation was carried with suitable execution parameters: The error tolerance on potential calculations was less than 0.3 V, the number of ion particle extracted from each sheath cell was more than 3, for example, $1000 > 29 \times 10 \times 3$. The igx code is written in FORTRAN77.

Results and Discussion

Evaluation of Simulation Codes

Initial simulation runs carried out to evaluate the codes were performed on the two-grid HiIsp-IT systems shown to scale with boundary conditions and grid potentials in Fig. 7. The node distance used was 0.149 mm. There is a large gap between the screen and accelerating grids (5.5 mm) to prevent electrical breakdown. The screen grid is relatively thick (1.5 mm) because a thin grid yielded a high accelerating grid impingement current I_{ac} under some operating conditions. The accelerating grid is thick (3 mm) and has a small aperture diameter (3.5 mm) compared to that of the screen grid (7 mm) to assure a long life. Furthermore, ions injected from sheath had an initial kinetic energy of 3 eV. Simulations were performed using both codes on an 800-MHz personal computer. Experimental results obtained on a grid set with 19 aperture pairs having the dimensions associated with Fig. 7 were available so that they could be compared to simulation results. An example of comparative results

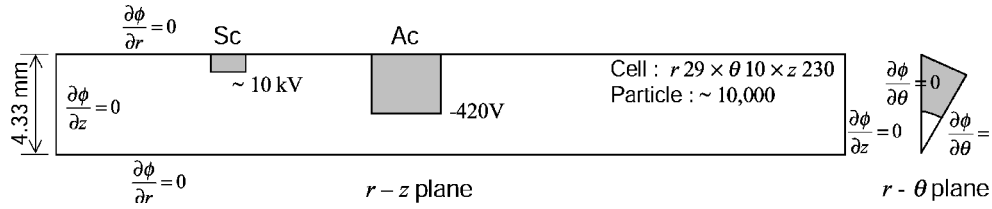

Fig. 7 HiIsp-IT grid system used for evaluation of codes.

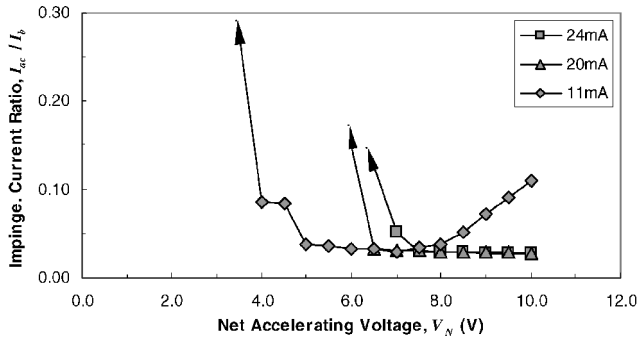

a) Experiment

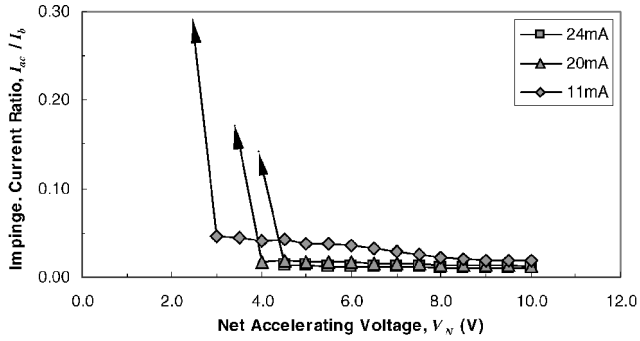

b) OPT code simulation

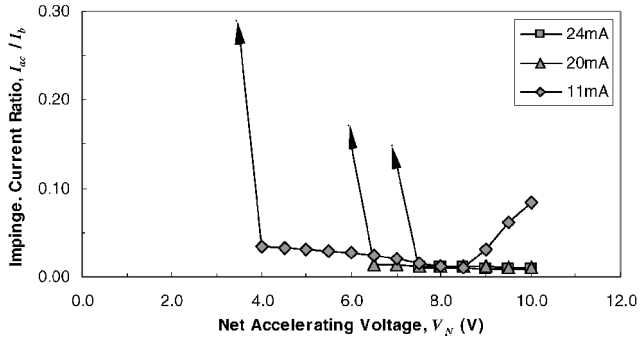

c) Simulation of igx code

Fig. 8 Impingement current comparisons.

obtained from this study is shown in Fig. 8. The experimental data shown were obtained by maintaining beam current constant and measuring the impingement current as the screen grid voltage was varied. Figures 8 show the variation in impingement to beam current ratio (I_{ac}/I_b) with net accelerating voltage V_N, and the following observations are made regarding the data.

OPT Code

Although the OPT code simulation is an appropriate analysis for conventional ion thrusters, comparison of Figs. 8a and 8b indicates it does not agree well with experimental data in this case. It appears that the code deficiency in this high-voltage case is caused by ions drawn through a screen grid hole from the region over the web between adjacent holes (point A in the r–θ plane of Fig. 3). The

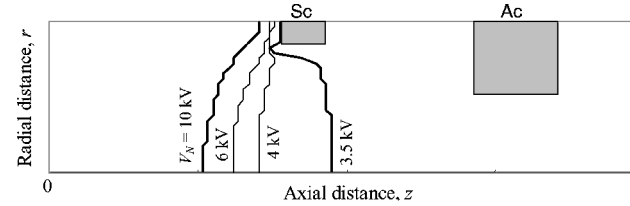

Fig. 9 Sheath position and shape.

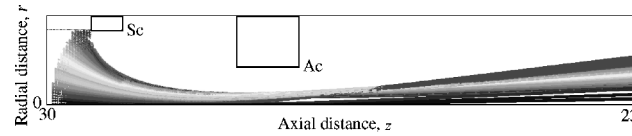

Fig. 10 Trajectory of ion beam.

inherent asymmetry associated with the effects of adjacent screen holes, which becomes important under high-voltage conditions, is not adequately modeled using a two-dimensional assumption when the sheath is far upstream.

igx Code

It is clear from a comparison of Figs. 8a and 8c that the igx code yields results that agree with the experimental data. Figure 9 shows the code prediction of changes in sheath position and shape as net accelerating voltage is varied when the beam current is 11 mA. As net accelerating voltage is increased, the sheath becomes increasingly concave upstream and farther from the screen grid (Fig. 9). On the other hand, the sheath is convex (ballooned downstream) and positioned farther downstream in the lowest voltage case. These results are consistent with crossover impingement at higher voltages and perveance-limited impingement when the voltage is lowest. These impingement phenomena were confirmed in our experiments. Figure 10 shows the trajectories of ions in the beam, and Fig. 11 shows the three-dimensional features of sheath and the cross section of the ion beam at the upstream plane of the acceleration grid at a typical low-perveance operating condition. Figure 12 shows the beamlet cross section determined by the foil erosion method[9] under conditions similar to those associated with the simulation, and it is in good agreement with the cross section of Fig. 11. Beamlet cross sections and effects of perveance on impingement current measured at other operating conditions[9] are also in good agreement with simulation results. Simulation using the igx code required 6–10 min per case and used ~40 MB of memory. These results suggest that the igx code simulation is better suited to the analysis and design of HiIsp-IT grid systems.

Variance of Simulation Results

To confirm its accuracy, the igx code simulation was executed 50 times under the same conditions without supplying an initial random number (a seed number used for random number generation). This was done because random numbers used in particle simulation can affect the result. Through the executions, it was confirmed that the variance of results had a range of ±3–5%, and the result was almost independent of the initial random number. Because the results of the igx code simulation also agree with the experimental data, as already mentioned, it is argued that the accuracy of igx simulation

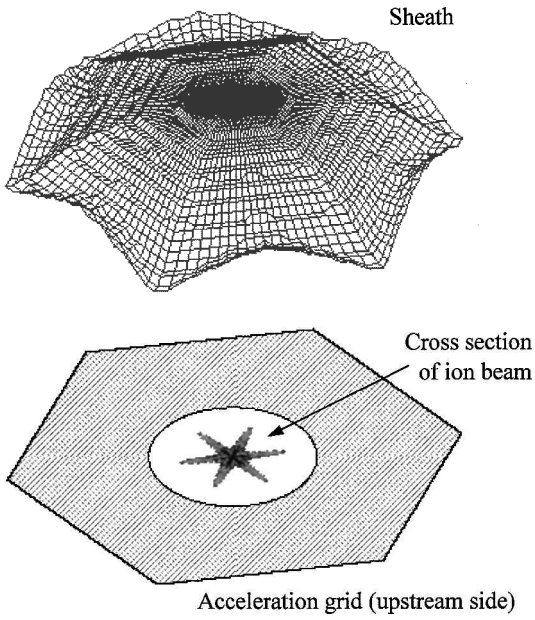

Fig. 11 Sheath and beamlet cross section.

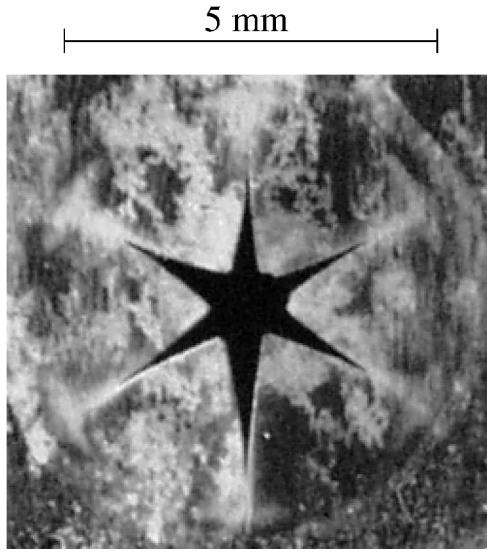

Fig. 12 Beamlet cross section determined by foil erosion method.

is suitable for evaluation of HiIsp-IT ion beam optics. Furthermore, it was determined that the accuracies depend strongly on perveance, and the accuracy was found to be within the aforementioned tolerance over the perveance range of $0.4–1.5 \times 10^{-9}$ A/V$^{3/2}$ under test conditions where the grid holes were aligned with 0.01–0.1 mm.

Discussion of Multiple-Grid Simulation Results

In view of the good agreement obtained between results from the igx code and experiments, it seemed reasonable to use it for analysis of HiIsp-IT multiple-grid options. Figure 13 shows the grid configurations that were simulated to obtain results that could be compared to each other and to the standard (type-O) configuration shown in Fig. 7.

Type A

This grid system is a conventional three-grid system with the same screen and acceleration grid dimensions as the type-O set. It was determined that the third (decelerating) grid, which is generally at a potential near 0 V, tended to facilitate charge-exchange ion flow away from the acceleration grid and into the downstream region. Numerical results showed 20–50% reductions in charge-exchange impingement currents depending on the beam current. Reductions

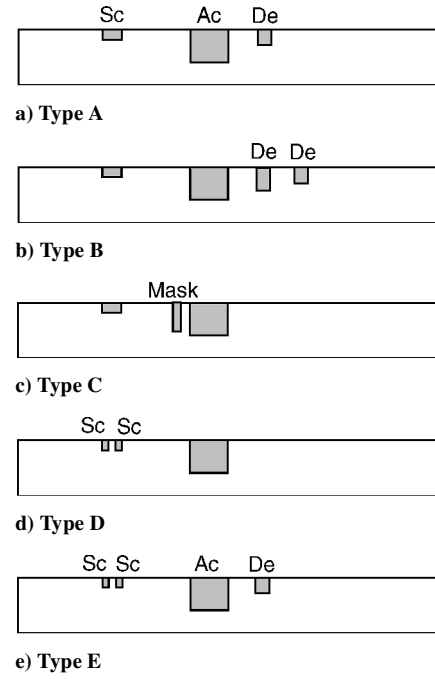

Fig. 13 Schematic of grid systems for HiIsp-IT applications.

in charge-exchange ion currents were observed on both the barrel and downstream surfaces of the acceleration grid aperture.

Type B

In this case, another decelerating grid is added to facilitate both a reduction in total impingement currents derived from charge-exchange reactions and management of ion beam trajectories in the downstream region. However, it was determined that this grid system gave rise to an increase in the total impingement current to all grids because it reduced the conductance for neutral flow and increased the charge-exchange reaction rate. It seemed that this grid system would not be well suited to HiIsp-IT applications.

Type C

Here a masking grid is added upstream of the accelerating grid to reduce ion impingement to the upstream surface of this grid. Although many simulations were examined in terms of the potential and dimensions of the mask, none were found that reduced the impingement current significantly below that for the type-O grid system.

Type D

This grid system has two screen grids. The second screen grid is used to enable management of ion beam trajectories. The potential of the second screen grid is greater than plasma potential (approximately the discharge voltage plus the first screen grid voltage). The spacing between the two screen grids is equal to the screen grid thickness for both this and the type-O system. Through numerical analysis, it was confirmed that this grid system was able to control (manage) the beam ion trajectories. Figure 14 shows how the ratios of thrusts and extracted beam currents (type D/type O) were affected by the ratio of voltages applied to the second and first screen grids. Figure 14 shows that the voltage on the second screen grid can be used to manage (collimate) the ion beam trajectories, thereby increasing the beam current and thrust factor. For example, the type-D grid system operated at a first screen grid voltage of 10 kV and a second screen grid voltage of 10.1 kV can extract approximately 1.15 times current of the type-O grid system operated at the screen grid voltage of 10.1 kV, and the former grid system also operates at a slightly greater thrust factor due to a reduction in divergence angle. It also yielded a modest reduction in impingement current. This option is complicated by the need to provide another power supply.

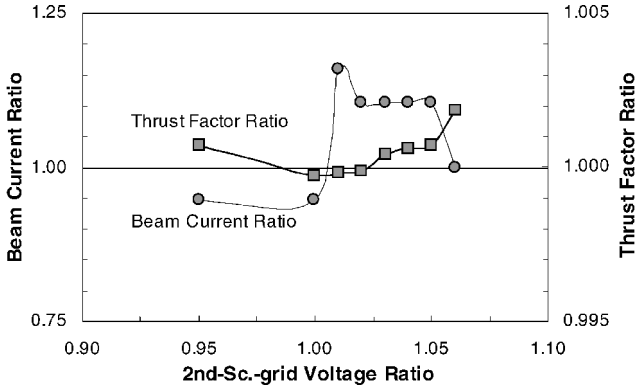

Fig. 14 Effects of voltage on second screen grid for type-D system.

Type E

This grid system is a combination of the type-A and type-D systems. Through parametric analysis, it was determined that the impingement current could be reduced while the thrust ratio and/or beam current could be increased with this option. This grid system is similar to one described by Aston.[10]

Although many cases were analyzed in this study, more detailed analysis and discussion of grid design options for HiIsp-IT grid systems is still needed. In addition, because an HiIsp-IT grid system has many designs, it is likely that this analysis also needs a high-efficiency optimization method such as the genetic algorithm.[11]

Conclusions

1) Modified OPT simulation is not in good agreement with experimental data measured on HiIsp-IT optics.

2) The new developed three-dimensional particle simulation code igx, which uses an energy-compensation method, a simplified definition approach, and high-speed coding, yields results that are in good agreement with experimental data.

3) Simulation using igx indicates the screen–screen–accelerating–decelerating grid system will yield well-focused beamlets, a reduced impingement current, and increased thrust.

4) More detailed analysis and discussion of grid design options for HiIsp-IT grid systems is needed.

References

[1]Whealton, J. H., McGaffey, R. W., and Stirling, W. L., "Ion Beam Extraction from a Plasma with Aberration Reduction by Method of Mutual Exclusion," *Journal of Applied Physics*, Vol. 52, No. 6, 1981, pp. 3787–3790.

[2]Hayakawa, Y., "Three-Dimensional Numerical Model of Ion Optics System," *Journal of Propulsion and Power*, Vol. 8, No. 1, 1992, pp. 110–117.

[3]Free, B., Owens, J. R., and Wilbur, P., "Variations of Triple-Grid Geometory and Potentials to Alleviate Accel Grid Erosion," 22nd International Electric Propulsion Conf., Paper IEPC-91-120, Oct. 1991.

[4]Nakano, M., and Arakawa, Y., "Ion Thruster Lifetime Estimation and Modeling Using Computer Simulation," *Proceedings of 26th International Electric Propulsion Conference*, The Japan Society for Aeronautical and Space Sciences, Tokyo, 1999, pp. 797–804.

[5]Okawa, Y., and Takegahara, H., "Particle Simulation on Ion Beam Extraction Phenomena in an Ion Thruster," *Proceedings of 26th International Electric Propulsion Conference*, The Japan Society for Aeronautical and Space Sciences, Tokyo, 1999, pp. 805–812.

[6]Muravlev, V. A., and Shagayda, A. A., "Numerical Modeling of Extraction Systems in Ion Thrusters," *Proceedings of 26th International Electric Propulsion Conference*, The Japan Society for Aeronautical and Space Sciences, Tokyo, 1999, pp. 910–917.

[7]Arakawa, Y., and Ishihara, K., "A Numerical Code for Cusped Ion Thruster," Proceedings of 22nd International Electric Propulsion Conf., Paper IEPC-91-118, Oct. 1991.

[8]Giaquinta, M., Shatah, J., and Varadhan, S. R. S., "Differential Equations: La Pietra 1996," *Proceedings of Symposia in Pure Mathematics*, Vol. 65, American Mathematical Society, New York, 1999, pp. 27–37.

[9]Wilbur, P. J., Miller, J., Farnell, C., and Rawlin, V. K., "A Study of High Specific Impulse Ion Thruster Optics," 27th International Electric Propulsion Conf., Paper IEPC-01-098, Oct. 2001.

[10]Aston, G., "High Efficiency Ion Beam Accelerator System," *Review of Science Instruments*, Vol. 52, No. 9, 1981, pp. 1325–1327.

[11]Nakayama, Y., and Wilbur, P. J., "The Feasibility of a Genetic-Algorithm-Based Ion Thruster Design Code," AIAA Paper 2001-3786, July 2001.